

## Investigation of vortex-induced vibration phenomenon in vertical long circular slender structure with non-uniform flows

\*M. Ghodsi Hasanabad; P. Fallah Lichaiee

\*Marine Industries Group, Science and Research Branch, Islamic Azad University, Tehran, Iran

Received 11 March 2013; revised 5 April 2013; accepted 7 May 2013

**ABSTRACT:** Analyzing the vortex-induced vibration of a slender marine structure with length to diameter ratio up to 200 is the objective of this study. This slender is free to move in both in-line and cross flow directions and immersed completely in water. Three different types of shear currents pass on it and cause to vibrate slender in different forms. Nowadays, these vibrations are very important for designers. In this study, 3D Finite difference method has been used to solve cable governing equations in a long slender with two hanged ends. The hydrodynamic forces, in the direction of in-line and cross-flow created by vortex shedding are simultaneously considered based on Morison equation. In a specified range of Reynolds number, the flow is in-line direction, but the results show riser oscillation in both in-line and cross flow directions. The results showed a good agreement with other researches in VIV with constant flow on it. Then non-uniform flows with profiles in real ocean currents were selected as inputs of this study. The results showed that small variations in velocity profiles and quantities can create significant differences in riser behavior.

**Keywords:** VIV, long slender, shear current, finite difference method

### INTRODUCTION

Vortex-induced vibration (VIV) is vibration caused by a change in the downstream pressure when fluids flow around slender marine structures. In laminar flows, vortices form at the back of the structure as the flow speed increase. Initially, symmetrical vortices occur and cause a displacement in the inline direction. As the flow speed increases, asymmetrical vortices begin to occur, and the structure vibrate in the inline and cross-flow directions simultaneously. When the flow speed exceeds a certain value, the displacement in the cross-flow direction becomes dominant and the vibration in the in-line direction is usually ignored. However, the displacement of the inline direction should be considered because in certain circumstances the displacement and the frequency in the inline direction may affect the fatigue life of the structure. The influence of in-line vibration has been reported by many researchers (Jauvtis and Williamson, 2004; Jeon and Gharib, 2001; Sarpkaya, 1995).

Jauvtis and Williamson (2004) have noticed a dramatic change in the cross-flow response as significant in-line motion appears, as the structure to

displaced fluid mass ratio is reduced below 6. An increase in the in-line to cross-flow natural frequency ratio induces changes as well, causing a larger cross-flow peak amplitude response (Dahl *et al.*, 2006; Lucor and Triantafyllou, 2008).

When vortex shedding frequency coincide with one of the structures natural frequencies, the structure exhibits resonant behavior. This phenomenon is referred to lock-in which is the most distinct feature of VIV and is observed in numerous laboratory experiments and flow simulations involving cables, cantilevers, bridge models and elastically held cylinders (Blackburn and Henderson, 1996; De Langre, 2006; Feng, 1968). Generally, lock-in is described as the ability of an elastic structure to control the shedding process in a bandwidth around its resonant frequency.

Short rigid cylinders possess well separated modal frequencies, which reduce the effects of modal interaction and cause single-mode lock-in to occur easily (Iwan and Jones, 1987). For long slender cylinders, which have many natural frequencies and as the frequency intervals between adjacent modes are very small, the cylinders are usually excited in multiple and higher modes (Brika and Laneville, 1993). In this case, lock-in is defined as the single

\*Corresponding Author Email: [m.ghodsi.h@gmail.com](mailto:m.ghodsi.h@gmail.com)  
Tel.: +9844865737

mode dominance, i.e. one mode has enough energy and prohibits competing modes from participating in the vibration (Vandiver et al., 1996). In many cases, no single mode dominates other competing modes, when non-lock-in occurs. Non-lock-in phenomenon is described in details by Kim et al., (1986).

In ocean environment, long slender cylinders are exposed to sheared flow over the length. In sheared flow, different modes are excited at different locations along the length of cylinder and each mode could be a potential factor, which influences the entire dynamic character of the cylinder. The response of the cylinder at any location along its length is seen as the superposition of each mode with corresponding participation factor. Thus in sheared flow, lock-in is defined as the circumstance in which the single mode dominates the response, whereas other modes are suppressed (Marcollo and Hinwood, 2006; Vandiver et al., 1996). Vandiver et al., (1996) presented two dimensionless parameters, which could be used to predict the occurrence of lock-in under the sheared flow condition. One is the number of potential modes within vortex shedding bandwidth and the other is the shear fraction, i.e. the ratio of variation of velocity to averaged velocity. Non-lock-in is highly probably to occur when the two parameters fall in ‘‘U’’ region (Fig. 1), beyond this region lock-in is more likely to happen. Marcollo and Hinwood (2006) observed that, in sheared flow, the response of the cylinder might vary from lock-in to non-lock-in, multi-mode behavior and IL motion was very important for predicting the CF lock-in. In

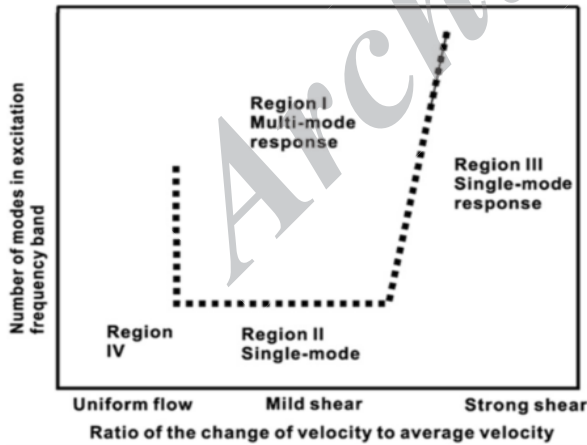


Fig. 1: Identification of lock-in (single mode) and multi-mode regions (Vandiver et al., 1996)

another experiment, lock-in phenomenon was not observed in well defined sheared flow and the responses were abundant in participating modes and frequency components (Lie and Kaasen, 2006). Vandiver et al. (1996) suggested that in the case of non-lock-in, several modes participate in the

vibration and no one mode can prevent competing mode from interacting with wake. Lock-in in sheared flow condition was also discussed by Bourguet et al., (2011). Generally the total root mean square (RMS) responses in the case of non-lock-in were remarkably lower than those in single-mode lock-in cases (Vandiver et al., 1996).

## MATERIALS AND METHODS

### Governing equation and numerical method

For the dynamic analysis of a slender marine structure, a three-dimensional governing equation is necessary to describe the structural behavior. Geometric and fluid nonlinearities must be considered in the derivation of the governing equation, in order to describe a nonlinear displacement induced by vortex shedding (Jung et al., 2012). The 3D dynamic equilibrium of a submerged long slender structure is governed by ten partial differential equations. These equations are provided in the Eqs.1 to 10 without further details on the derivation procedure. For more details refer to the works of Howell (1992), Burgess (1993), Triantafyllou (1994) and Tjavaras et al. (1998).

$$m \left( \frac{\partial u}{\partial t} + w \frac{\partial \theta}{\partial t} - v \frac{\partial \phi}{\partial t} \cos \theta \right) = \frac{\partial T}{\partial s} + S_b \Omega_n - S_n \Omega_b - W_0 \cos \phi \cos \theta + R_t \quad (1)$$

$$m \left( \frac{\partial v}{\partial t} + \frac{\partial \phi}{\partial t} (u \cos \theta + w \sin \theta) \right) + m_a \frac{\partial v}{\partial t} = \frac{\partial S_n}{\partial s} + \Omega_b (T + S_b \tan \theta) + W_0 \sin \phi + m_i \frac{\partial U_n}{\partial t} + R_n \quad (2)$$

$$m \left( \frac{\partial w}{\partial t} - v \frac{\partial \phi}{\partial t} \sin \theta - u \frac{\partial \theta}{\partial t} \right) + m_a \frac{\partial w}{\partial t} = \frac{\partial S_b}{\partial s} - S_n \Omega_b \tan \theta - T \Omega_n - W_0 \cos \phi \sin \theta + m_i \frac{\partial U_b}{\partial t} + R_b \quad (3)$$

$$EI \frac{\partial \Omega_n}{\partial s} = -EI \Omega_b^2 \tan \theta + S_b \left( 1 + \frac{T}{EA} \right)^3 \quad (4)$$

$$EI \frac{\partial \Omega_b}{\partial s} = EI \Omega_n \Omega_b \tan \theta - S_n \left( 1 + \frac{T}{EA} \right)^3 \quad (5)$$

$$\frac{\partial u}{\partial s} + \Omega_n w - \Omega_b v = \frac{1}{EA} \frac{\partial T}{\partial t} \quad (6)$$

$$\frac{\partial v}{\partial s} + \Omega_b (u + w \tan \theta) = \left( 1 + \frac{T}{EA} \right) \frac{\partial \phi}{\partial t} \cos \theta \quad (7)$$

$$\frac{\partial w}{\partial s} - \Omega_b v \tan \theta - \Omega_n u = - \left( 1 + \frac{T}{EA} \right) \frac{\partial \theta}{\partial t} \quad (8)$$

$$\Omega_n = \frac{\partial \theta}{\partial s} \quad (9)$$

$$\Omega_b = \frac{\partial \phi}{\partial s} \cos \theta \quad (10)$$

where (s) is the structure length coordinate, subscripts t, n, and b directions in the local coordinate system, T

is effective tension of the structure, S is shear force,  $u, v$  and  $w$  velocity of structure in local directions,  $U_n, U_b$  are fluid velocity in local coordinates,  $\Omega$  is curvature,  $m$  is mass per unit length,  $W_0$  is weight per unit length in water,  $R$  is fluid drag force,  $m_a, m_i$  are added mass and inertia mass per unit length,  $E$  is Young's modulus,  $A$  is the cross sectional area of the structure and  $I$  is inertia moment of cross section. The excitation forces in the inline and cross-flow directions induced by the vortex shedding are given in Eqs.11 and 12:

$$F_{inline} = \frac{1}{2} \rho C_{inline} D U^2 \sin(2\pi f_{inline} t + \phi_{inline}) \quad (11)$$

$$F_{cross} = \frac{1}{2} \rho C_{cross} D U^2 \sin(2\pi f_{cross} t + \phi_{cross}) \quad (12)$$

Where  $F_{inline}$  is the excitation force in the inline direction,  $F_{cross}$  is excitation force in the cross-flow direction,  $\rho$  is water density,  $C_{inline}$  is drag coefficient in global coordinates,  $C_{cross}$  is lift coefficient in global coordinates,  $f_{inline}$  is inline force frequency,  $f_{cross}$  is cross-flow force frequency,  $\phi_{inline}$  is phase angle between inline force and displacement,  $\phi_{cross}$  is phase angle between cross-flow force and displacement.

In this study the global coordinate is labeled as X, Y, Z and this coordinate system is fixed in space. The local one is fixed on riser element and is labeled as t, n, b. It is necessary to transform between two coordinates through a set of rotations known as Euler angles. The rotation sequence chosen in this work is as follows: First rotate the local axes by the angle  $\phi$  about the Z-axis, then rotate them the angle  $\theta$  about the new Y-axis. We neglected torsion rigidity of the cable, so the rotation about the new Z-axis was not considered. These rotations can be expressed in matrix form as Eq. 13 (Jung et al., 2005):

$$\begin{bmatrix} t \\ n \\ b \end{bmatrix} = \begin{bmatrix} \cos \phi \cos \theta & \sin \phi \cos \theta & -\sin \theta \\ -\sin \phi & \cos \phi & 0 \\ \cos \phi \sin \theta & \sin \phi \sin \theta & \cos \theta \end{bmatrix} \begin{bmatrix} X \\ Y \\ Z \end{bmatrix} \quad (13)$$

The direction of the coordinate system is given in Fig. 2.

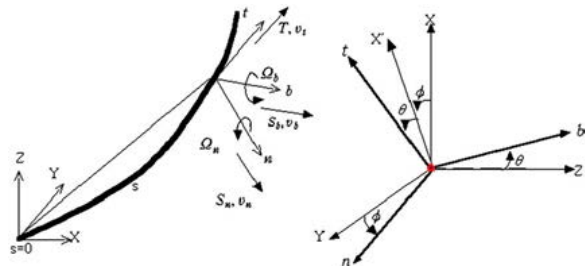


Fig. 2: Coordinate systems (left) and Euler rotation sequence (right)

These equations can be expressed in a matrix form as Eq. 14:

$$K \frac{\partial Y}{\partial s} = M \frac{\partial Y}{\partial t} + F \quad (14)$$

Where, Y and F are vector matrices and K and M are all 10· 10 size of square matrices in Eq. 14.

$$Y = [T \ S_n \ S_b \ u \ v \ w \ \phi \ \theta \ \Omega_n \ \Omega_b]^T \quad (15)$$

$$F = \begin{bmatrix} -S_b \Omega_n + S_n \Omega_b + W_0 \cos \phi \cos \theta - R_t \\ -\Omega_b (T + S_b \tan \theta) - W_0 \sin \phi + m_i \frac{\partial U_n}{\partial t} - R_n \\ S_n \Omega_b \tan \theta + T \Omega_n + W_0 \cos \phi \sin \theta + m_i \frac{\partial U_b}{\partial t} - R_b \\ -\Omega_n w + \Omega_b v \\ -\Omega_b (u + w \tan \theta) \\ \Omega_b v \tan \theta + \Omega_n u \\ \Omega_b \\ \Omega_n \\ -EI \Omega_b^2 \tan \theta + S_b \left(1 + \frac{T}{EA}\right)^3 \\ EI \Omega_n \Omega_b \tan \theta - S_n \left(1 + \frac{T}{EA}\right)^3 \end{bmatrix} \quad (16)$$

The nonzero components of M are as follows:  $M(1,4) = m$ ,  $M(1,7) = -mv \cos \theta$ ,  $M(1,8) = mw$ ,  $M(2,5) = m + m_a$ ,  $M(2,7) = mu \cos \theta + mw \sin \theta$ ,  $M(3,6) = m + m_a$ ,  $M(3,7) = -mv \sin \theta$ ,  $M(3,8) = -mu$ ,  $M(4,1) = \frac{1}{EA}$ ,  $M(5,7) = \left(1 + \frac{T}{EA}\right) \cos \theta$ ,  $M(6,8) = -\left(1 + \frac{T}{EA}\right)$ . In the case of K matrix, the diagonal components are as follows but other components are zero.

$K(1,1) = K(2,2) = K(3,3) = K(4,4) = K(5,5) = K(6,6) = K(8,8) = 1$ ,  $K(7,7) = \cos \theta$ ,  $K(9,9) = K(10,10) = EI$ .

For solving these equations, at first, the structure is discretized into  $n$  nodes separating by  $\Delta s$  and time is divided into a series of time steps of length  $\Delta t$ . Using central finite differences, evaluating Eq. 4 at mid-node of  $k+1/2$  and the time of  $i+1/2$  gives:

$$\begin{aligned} & [K_{k+1}^{i+1} + K_k^{i+1}] \frac{Y_{k+1}^{i+1} - Y_k^{i+1}}{\Delta s} \\ & + [K_{k+1}^i + K_k^i] \frac{Y_{k+1}^i - Y_k^i}{\Delta s} = \\ & [M_{k+1}^{i+1} + M_k^{i+1}] \frac{Y_{k+1}^{i+1} - Y_k^{i+1}}{\Delta t} \\ & + [M_k^{i+1} + M_k^i] \frac{Y_k^{i+1} - Y_k^i}{\Delta t} + F_{k+1}^{i+1} \\ & + F_k^{i+1} + F_{k+1}^i + F_k^i \end{aligned} \quad (17)$$

Equations given in this research are nonlinear, so it is necessary to solve the equations at each time step

iteratively. In this study, a NewtonRaphson iteration scheme and steepest decent method were applied. The numerical algorithm was validated with the experimental study by Jung *et al.*, (2005).

## RESULTS AND DISCUSSION

In this research, the vibration behavior of flexible risers has been investigated due to VIV in shear currents.

Table 1: Geometrical and mechanical properties of the riser

Length	10	meter
Outer diameter	0.02	meter
Inner diameter	0.01	meter
Elastic modulus	$1 \times 10^{10}$	Pascal
Mass per unit volume	1250	kg/m <sup>3</sup>
Boundary condition (bottom, top)	Hing	

For this purpose, 3 different velocity profiles (Fig. 3) in depth direction have been used. These velocity profiles were: 1) linear with maximum speed of 0.5 m/s on the free surface and minimum speed of 0.1 m/s on the riser end, 2) exponential with mentioned speeds, and 3) linear in 55% of top section of the riser and zero in end section of the riser. These velocity profiles were chosen due to their applications in marine and sea currents (Bourguet *et al.*, 2012; HueraHuarte, 2006).

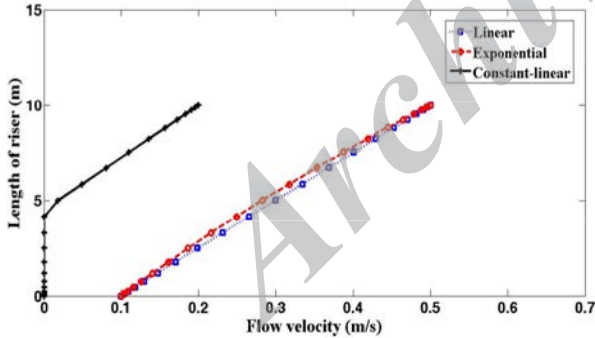


Fig. 3: Three velocity profile

Natural frequencies of tensioned beam were obtained using Eqs. 18 to 20:

$$\omega_b = \left(\frac{n\pi}{L}\right)^2 \sqrt{\frac{EI}{m + m_a}} \quad (18)$$

$$\omega_T = \left(\frac{n\pi}{L}\right) \sqrt{\frac{T}{m + m_a}} \quad (19)$$

$$\omega^2 = \omega_b^2 + \omega_T^2 \quad (20)$$

Lock-in velocity in each vibration mode can be calculated using strouhal relation (Eq. 21) and considering equality of vortex shedding frequency and structure natural frequency. These quantities have been illustrated in Table 2.

$$st = \frac{f_x D}{U} \quad (21)$$

In which  $st$ ,  $f_x$ ,  $D$ , and  $U$  are Struhal number, vortex shedding frequency, outer diameter of riser, and current velocity, respectively. Struhal number is 0.2 for a structure with circle cross section in wide range of Reynolds number (Belvin, 1977). This number has been considered for the present study.

Table 2: natural frequency and lock-in velocity for in-line and cross flow direction

Mode	$f_n$ (Hz)	$U_{lock-in\ crossflow}$ (m/s)	$U_{lock-in\ inline}$ (m/s)
1 <sup>st</sup>	0.423	0.042	0.0212
2 <sup>nd</sup>	1.016	0.1016	0.0508
3 <sup>rd</sup>	1.875	0.187	0.0938
4 <sup>th</sup>	3.035	0.3035	0.1517
5 <sup>th</sup>	4.51	0.451	0.2255

The results of this study have been compared with the results of Jung *et al.*, (2012) to validate the results (Figs. 4 and 5). Fig. 4 shows the riser displacement in cross flow direction for 3 points: 1/3 from riser end, the middle of the riser, and 2/3 from riser end. Fig. 4-a shows the results of this study while figure 4-b shows the results of previous study (Jung *et al.* 2012). In order to present the results in an understandable format, all results were processed using fast Fourier transform. As shown in Fig. 4, there is a good accordance between the displacement of middle point in this study and previous results. The period of middle point in Fig. 4-a seems larger than the same parameter in Fig. 4-b, but it is due to FFT application for data and there is acceptable coincidence in unprocessed data. The major difference between Figs. 4-a and 4-b is in point 3 (2/3 from the end), in which the amplitude of oscillation is about 2 times larger than the study of Jung *et al.* (2012). It can be due to some little differences between the geometrical and mechanical properties in these two studies. Also, this comparison was made for 0.05 m/s current velocity in Fig. 5. Generally, it can be said that the results of this study are in good agreement with similar studies.

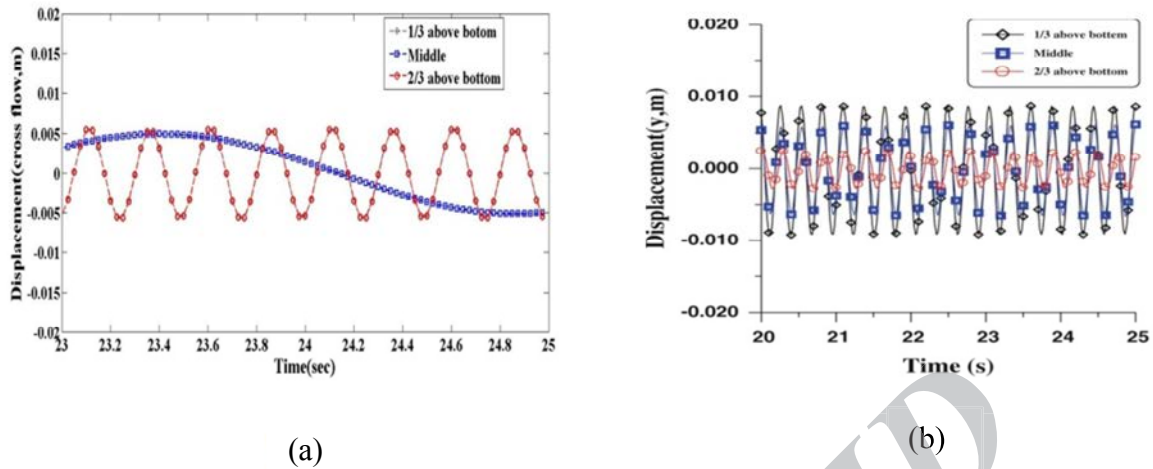


Fig. 4: Time history of nodes displacements in 1/3, middle, and 2/3 of riser length from the bottom. (a) Present study (b) Jung's study (Jung *et al.*, 2012) in uniform flow with velocity of 0.4m/s

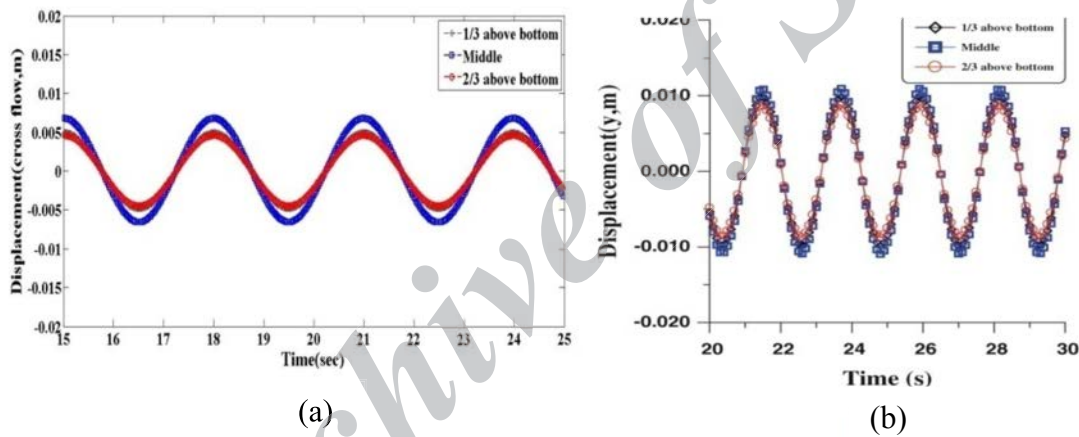


Fig. 5: Displacement time history of points 1/3, middle and 2/3 from bottom For: (a) =this research and (b) = (Jung *et al.*, 2012) in uniform flow with velocity of 0.05m/s

In Fig. 6, the vibration of structure has been shown in 3 different velocity profiles. Figs. 6-a, 6-b, and 6-c are related to linear profile, exponential profile, and constant-linear profile, respectively.

As shown in Fig. 3, the minimum and maximum velocities are equal in linear and exponential profiles and two profiles are close together. However, Fig. 6 shows larger amplitude for exponential profile than linear profile. Because, in Fig. 6-b less vibration modes are contributed relative to Fig. 6-a. In fact, the structure's behavior is completely non-lock in according to Fig. 6-a.

Fig.7 shows the displacement of middle point of structure in the inline direction for three velocity

Profiles Fig. 7 demonstrates middle point displacement of structure under 3 velocity profiles respect to time. The largest displacement is related to linear profile. It seems reasonable, because the velocity magnitude in linear profile in each height of riser is more than 2 other profiles.

The displacement of riser's points located on 1/3 from riser's end, the middle of riser and 2/3 from riser's end under linear and exponential currents in cross flow direction are presented in Fig. 8. Because of near lock-in behavior of structure under the exponential velocity profile, displacements of all three points due to this velocity profile are larger than same points in other currents (Figs. 8 and 9).

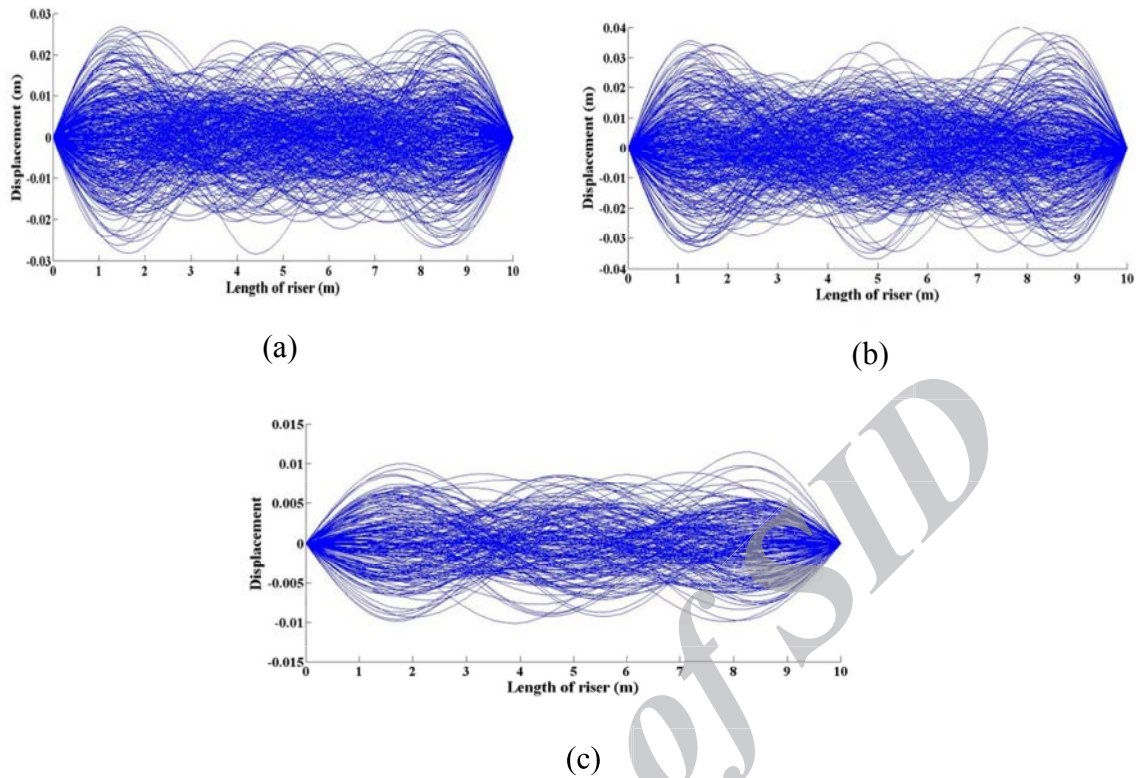


Fig. 6: Snapshot of configuration in XZ coordinate. (a) relative to linear velocity profile (b) Relative to exponential velocity profile and (c) relative to constant-linear velocity profile.

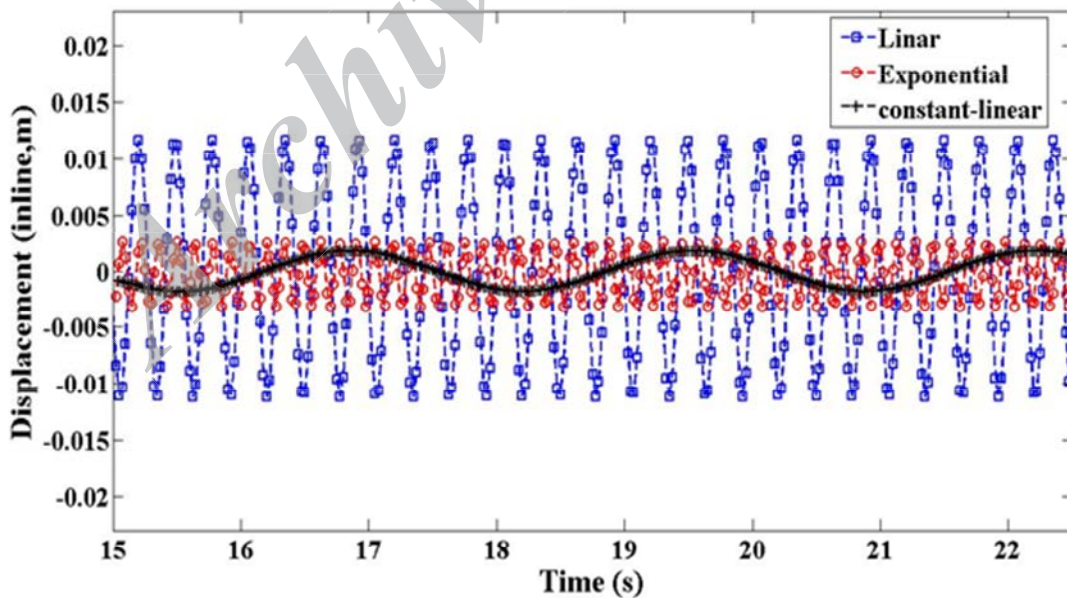


Fig. 7: In-line displacement of the middle point of structure for 3 velocity profiles

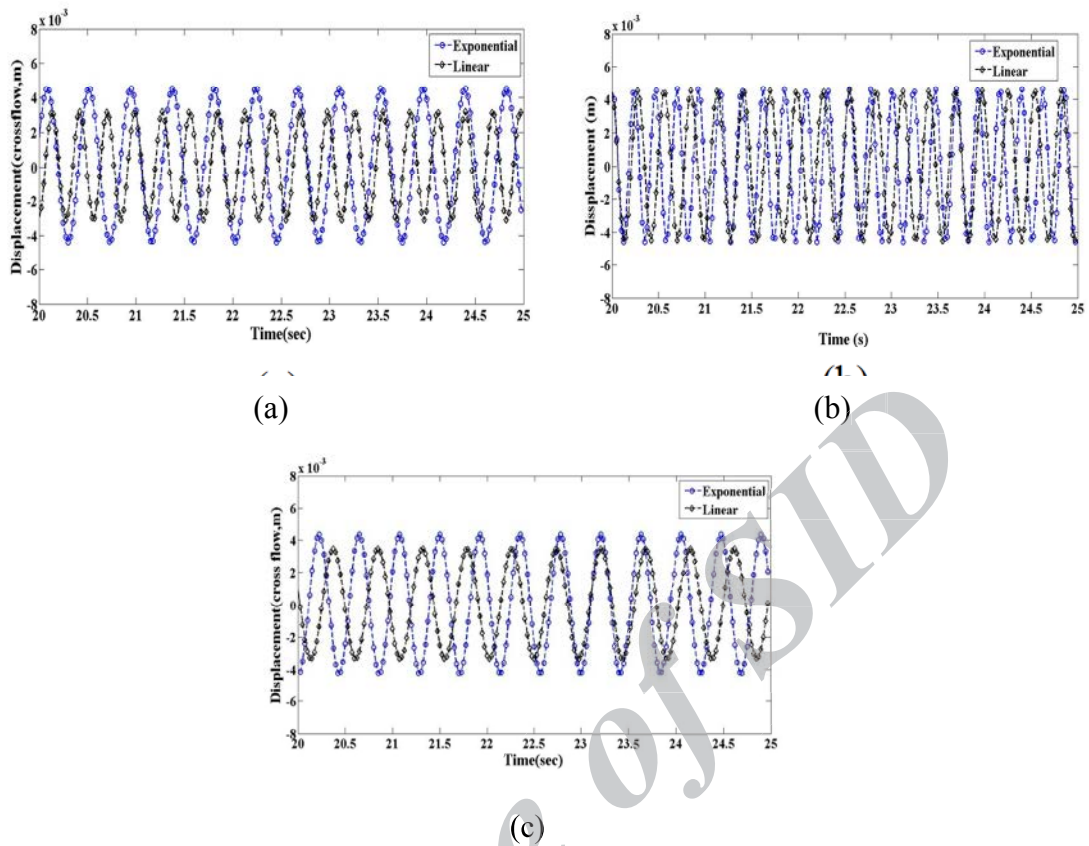


Fig. 8: crossflow displacement time history of points (a) 1/3, (b) middle and (c) 2/3 from bottom for linear and exponential velocity profiles.

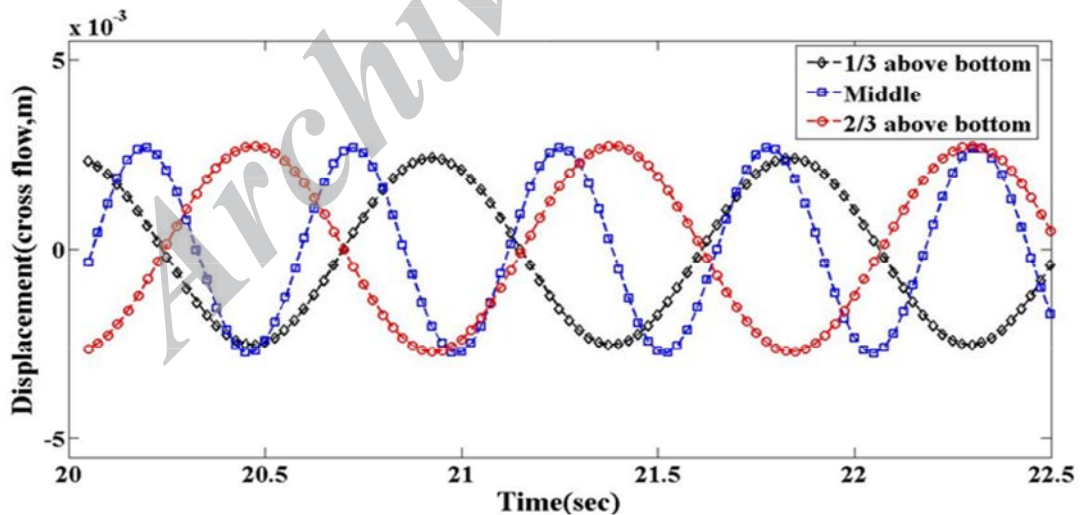


Fig. 9: crossflow displacement time history of points (a) 1/3, (b) middle and (c) 2/3 from bottom for constant-linear velocity profiles.

**CONCLUSION**

The results showed that in-line displacements of risers are increased by current velocity increment, but cross flow displacements of risers do not follow this procedure. In specified range of Reynolds number vortex shedding is occurred. In this situation, natural

frequencies of structure and induced frequencies of currents are very important in vibration behavior of structure. In some frequencies, lock-in phenomenon is occurred and the amplitude of cross flow vibration increases, considerably. This phenomenon can be occurred by small varying in current velocity or

current pattern. On the other hand, riser oscillation in cross direction is very sensitive to velocity in magnitude and pattern. Therefore, recording of current velocity in depth direction should be done precisely for riser's design. Also, this vibration causes fatigue in structure and should be considered in design and a specified solution should be chosen for each riser and current properties.

The cross flow displacements of riser due to linear-constant velocity profile are smaller than others. It is interesting that in-line displacements by linear-constant flow are nearly equal to exponential flow despite its lower current velocity.

## REFERENCES

- Blackburn, H. M.; Henderson, R. D., (1996). Lock-in behavior in simulated vortex-induced vibration. *Experimental Thermal and Fluid Science* 12, 184-189.
- Blevin, R. D., (1977). *Flow induced vibration*. Van Nostrand Reinhold, New York.
- Bourguet, R.; Karniadakis, G. E.; Triantafyllou, M. S., (2011). Lock-in of the vortex-induced vibrations of a long tensioned beam in shear flow. *Journal of Fluids and Structures*, 27, 838-847.
- Brika, D; Laneville, A., (1993). Vortex-induced vibrations of a long flexible circular-cylinder. *Journal of Fluid Mechanics* 250, 481-508.
- Burgess, J. J., (1993). Bending stiffness in a simulation of undersea cable deployment. *International Journal of Offshore and Polar Engineering*, 3, 197-204.
- Dahl, J. M.; Hover, F. S.; Triantafyllou, M. S., (2006). Two-degree-of-freedom vortex-induced vibrations using a force assisted apparatus. *Journal of Fluids and Structures*, 22, 807-818.
- De Langre, E., (2006). Frequency lock-in is caused by coupled-mode flutter. *Journal of Fluids and Structures* 22, 783-791.
- Feng, C. C., (1968). *The Measurement of Vortex Induced Effects in Flow Past Stationary and Oscillating Circular and d-Section Cylinders*. Master's Thesis, Department of Mechanical Engineering, the University of British Columbia, Canada.
- Howell, C. T., (1992). Investigation of the dynamics of low tension cables. PhD Thesis, Massachusetts Institute of Technology, Cambridge, Massachusetts.
- Iwan, W. D., Jones, N. P., (1987). On the vortex-induced oscillation of long structural elements. *Journal of Energy Resources Technology* 109, 161-167.
- Jauvtis, N.; Williamson, C. H. K., (2004). effect of two degrees of freedom on vortex-induced vibration at low mass and damping. *Journal of Fluid Mechanics* 509, 23-62.
- Jeon, D., Gharib, M., (2001). On circular cylinders undergoing two-degree-of-freedom forced motions. *Journal of Fluids and Structures* 15, 533-541.
- Jung, D.; Kim, H.; Shin, S., (2012). Characteristics of VIV in multi-degree of freedom tensioned beams using a numerical method. *Journal of marine science and technology*.
- JUNG, D. H., PARK, H. I., KOTERAYAMA, W. & KIM, H. J. 2005. Vibration of highly flexible free hanging pipe in calm water. *Ocean Eng*, 32, 1726-1939.
- Kim, Y. H., Vandiver, J. K., Hollar, R., (1983). Vortex-induced vibration and drag coefficients of long cables subjected to sheared flows. *Journal of Energy Resources Technology*, 107, 77-83.
- Lie, H.; Kaasen, K. E., (2006). Modal analysis of measurements from a large-scale VIV model test of a riser in linearly sheared flow. *Journal of Fluids and Structures*, 22, 557-575.
- Lucor, D.; Triantafyllou, M. S., (2008). Parametric study of a two degree-of-freedom cylinder subject to vortex-induced vibrations. *Journal of Fluids and Structures*, 24, 1284-1293.
- Marcollo, H.; Hinwood, J. B., (2006). On shear flow single mode lock-in with both cross-flow and in-line lock-in mechanisms. *Journal of Fluids and Structures* 22, 197-211.
- Sappkaya, T., (1995). Hydrodynamic damping, flow-induced oscillations, and biharmonic response. *Journal of Offshore Mechanics and Arctic Engineering*, 117, 232-238.
- Tjavaras, A. A.; Zhu, Q.; Liu, Y.; Triantafyllou, M. S.; Yus, D. K. P., (1998). The mechanics of highly extensible cables. *Journal of Sound and Vibration*, 213, 709-737.
- Triantafyllou, M. S., (1994). Cable mechanics for moored floating structures. *Proceedings of the 7th International Conference on the Behaviour of Offshore Structures (BOSS 1994)*, Boston, Massachusetts, 2, 57-77.
- Vandiver, J. K.; Allen, D.; Li, L., (1996). The occurrence of lock-in under highly sheared conditions. *Journal of Fluids and Structures* 10, 555-561.

### How to cite this article: (Harvard style)

Ghods Hasanabad, M.; Fallah Lichaiee, P., (2013). Investigation of VIV phenomenon in vertical long circular slender structure with non-uniform flows. *Int. J. Mar. Sci. Eng.*, 3 (3), 105-112.